Crystal structures and vibrational spectra of L-argininium(2+) bis(tetrafluoroborate) and L-argininium(2+) bis(perchlorate)

R.P. Sukiasyan, K.Yu. Suponitsky, A.K. Atanesyan, A.A. Danghyan, A.A. Hovhannisyan, A.M. Petrosyan

PII:	S1386-1425(19)31172-2
DOI:	https://doi.org/10.1016/j.saa.2019.117782
Reference:	SAA 117782
To appear in:	*Spectrochimica Acta Part A: Molecular and Biomolecular Spectroscopy*
Received date:	15 July 2019
Revised date:	9 November 2019
Accepted date:	10 November 2019

Please cite this article as: R.P. Sukiasyan, K.Y. Suponitsky, A.K. Atanesyan, et al., Crystal structures and vibrational spectra of L-argininium(2+) bis(tetrafluoroborate) and L-argininium(2+) bis(perchlorate), *Spectrochimica Acta Part A: Molecular and Biomolecular Spectroscopy*(2019), https://doi.org/10.1016/j.saa.2019.117782

Crystal structures and vibrational spectra of *L*-argininium(2+) bis(tetrafluoroborate) and *L*-argininium(2+) bis(perchlorate)

R.P. Sukiasyan [a], K.Yu. Suponitsky [b,c], A.K. Atanesyan [a], A.A. Danghyan [a],
A.A. Hovhannisyan[d], A.M. Petrosyan [a][1]

[a] *Institute of Applied Problems of Physics, NAS of Armenia25 Nersessyan Str., 0014 Yerevan, Armenia*
[b] *A.N. Nesmeyanov Institute of Organoelement Compounds, Russian Academy of Sciences, 28 Vavilova Str., Moscow, Russian Federation*
[c] *Plekhanov Russian University of Economics, Stremyanny per. 36, Moscow, Russian Federation*
[d] *Molecule Structure Research Centre, NAS of Armenia, 26 Azatutyan Ave., 0014, Yerevan, Armenia*

Abstract

In the present work crystal structures of (*L*-$ArgH_2$)$(BF_4)_2$ (I) and (*L*-$ArgH_2$)$(ClO_4)_2$ (II) isostructural salts have been determined. They crystallize in triclinic system with space group *P*1 and Z=1. Structure features of the (I) and (II) were compared with respective data of previously known (*L*-ArgH)(BF_4) and (*L*-ArgH)(ClO_4) salts with singly charged *L*-argininium(+) cation. Infrared and Raman spectra of the (I) and (II) are compared with spectra of (*L*-ArgH)(BF_4) and (*L*-ArgH)(ClO_4) salts. The presence of cation and anions and hydrogen bonds between them are reflected in the IR and Raman spectra. The crystals (I) and (II) exhibit second harmonic generation activity.

Keywords: Salts of L-arginine; tetrafluoroborate; perchlorate; crystal structure; vibrational spectra

1. Introduction

Crystalline salts of *L*-arginine are interesting as promising nonlinear optical materials [1]. After revealing the promising nonlinear optical properties of *L*-arginine phosphate monohydrate (LAP) [2], the work of Monaco et al. [3] was the first in which systematic search for its new chemical analogs was carried out. The authors investigated the symmetry, unit cell parameters as well as linear and nonlinear optical properties of some previously known and new crystals. An attempt to obtain an arsenate analog of LAP led to the discovery of the *L*-Arg.$2H_3AsO_4$ crystal, which proved to be a salt with doubly charged *L*-argininium(2+) cation,

---

[1] Corresponding author: E-mail addresses: aram.m.petrosyan@gmail.com, apetros@iapp.sci.am (A.M. Petrosyan)

(L-$ArgH_2$)(H_2AsO_4)$_2$ [4]. In [5,6] it was shown that an entire class of salts with L-argininium(2+) cation exists: (L-$ArgH_2$)$Cl_2.H_2O$, (L-$ArgH_2$)$Br_2.H_2O$, (L-$ArgH_2$)(IO_3)$_2$, (L-$ArgH_2$)(NO_3)$_2$, (L-$ArgH_2$)(H_2PO_4)$_2$. Monaco et al. [3] among other crystals obtained also orthorhombic crystals of (L-ArgH)(BF_4) and (L-ArgH)(ClO_4) with close unit cell parameters, but with optically negative and positive signs, respectively. In [7,8] their crystal structures were determined. Later these crystals were grown and investigated by different authors [9-16]. The first attempt to obtain the crystal (L-$ArgH_2$)(ClO_4)$_2$ with doubly charged L-argininium(2+) cation at usual conditions (in air at room temperature) was unsuccessful [5]. Later [17] the existence of this salt was confirmed by IR and Raman spectra and it was found that the cause of the previous unsuccessful attempt was the high hygroscopicity of the crystal. By analogy, one might expect that the crystal (L-$ArgH_2$)(BF_4)$_2$ also can be obtained similarly. Although hygroscopicity is undesirable property for application of nonlinear optical crystals, obtaining and investigation of these crystals is of interest from chemical, structural and vibrational spectroscopic points of view.

In the present paper structures of (L-$ArgH_2$)(BF_4)$_2$ (**I**) and (L-$ArgH_2$)(ClO_4)$_2$ (**II**) crystals have been determined. The IR and Raman spectra of the (**I**) and (**II**) were recorded and compared with respective results of (L-ArgH)(BF_4) and (L-ArgH)(ClO_4) crystals.

2. Experimental

As initial reagents we used L-arginine purchased from “Sigma” and HBF_4, $HClO_4$ acids (“Reakhim”), which are 40% and 57% solutions, respectively. The crystals of (**I**) and (**II**) were synthesized from aqueous solution containing L-arginine and respective HBF_4, $HClO_4$ acids in 1:2 molar ratio in closed vessel in presence of silica gel as water vapors absorber at room temperature. In a typical experiment for synthesis of the (**I**) 3 g of L-arginine was dissolved in 5 ml water and added to 3.02 g (5 ml) of HBF_4 solution. Crystallization started at *ca*. 4 ml of the solution. For synthesis of the (**II**) 3 g of L-arginine was dissolved in 5 ml water and added to 3.46 g (4 ml) of $HClO_4$. For crystal growth of (**I**) and (**II**) 1:1.5-1:3 molar ratios region was checked for optimizing and decreasing of viscosity of solution at room temperature. For crystal growth of (**I**) 1:3 molar ratio was used: 9 g of L-arginine was dissolved in 15 ml water and added to 13.61 g (20 ml) of HBF_4 solution. Using a seed is very desirable. Crystallization started at *ca*. 20 ml of solution. For the (**II**) 1:2.5 molar ratio was used: 9 g (L-Arg) was dissolved in 15 ml water and added to 12.975 g (15 ml) of $HClO_4$. Crystallization started at ca. 15 ml of solution.

The crystals are hygroscopic, but they are easy to grow. By this reason under normal conditions the crystals are not formed by evaporation. In Fig. 1 obtained crystals are shown.

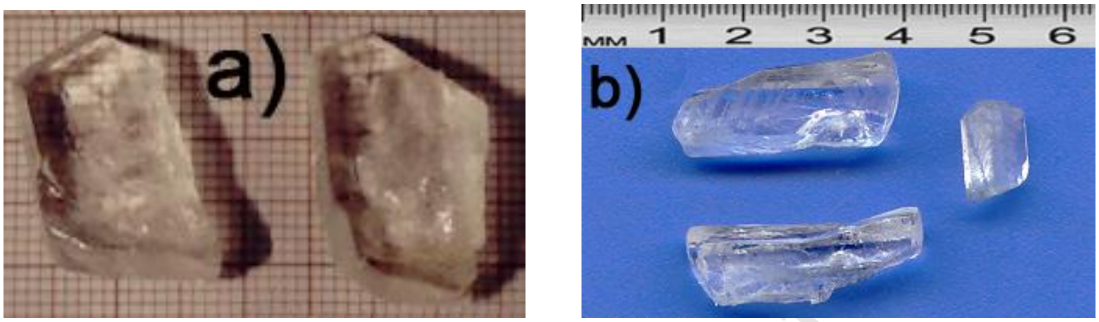

Fig. 1. The as-grown crystals of (**I**) a) and (**II**) b).

Attenuated total reflection Fourier-transform infrared spectra (FTIR ATR) were registered by a Nicolet 5700 spectrometer (ZnSe prism, Happ-Genzel apodization, ATR distortion is corrected, number of scans 32, resolution 4 cm^{-1}). Part of the IR spectrum in the region 500–400 cm^{-1} was taken from FTIR spectra registered with Nujol mull (4000–400 cm^{-1}, number of scans 32, resolution 2 cm^{-1}).

Fourier-transform Raman spectra were registered by NXR FT-Raman Module of a Nicolet 5700 spectrometer ($Nd:YVO_4$ laser with 976 nm wavelength, number of scans: 256, laser power at the sample: 0.43 W, resolution 4 cm^{-1}) at room temperature.

Second harmonic generation was checked by direct observation on the crystal using a pulsed YAG:Nd laser with passive Q-switching (duration of pulses 20 ns, repetition rate 8 Hz) [18].

The X-ray intensity data of the (**I**) and (**II**) single crystals were measured using Smart APEX2 CCD diffractometer, equipped with a graphite monochromator and using Mo-Kα (λ=0.71073 Å) radiation at 120K. Collected data were processed by the SAINT и SADABS programs [19]. The structures were solved by the direct methods and refined by the full-matrix least-squares procedure against F^2 in anisotropic approximation. The refinement was carried out with the SHELXTL program [20]. The details of data collection and crystal structures refinement of isostructural (**I**) and (**II**) salts are summarized in Table 1. Some oxygen atoms of the ClO_4^- anions are disordered over two positions (see Fig 1S in Supporting Info). Both parts were refined anisotropically. The ratio of the disordered parts was also refined and converged to 0.58(5):0.42(5). Further crystallographic data have been deposited with the Cambridge

Crystallographic Data Centre and can be obtained free of charge via www.ccdc.cam.ac.uk/conts/retrieving.html (or from the Cambridge Crystallographic Data Centre, 12 Union Road, Cambridge CB2 1EZ, UK; fax: +44 1223 336033), citing the title of this paper and the CCDC nos. 1897677 for **I** and 1897678 for **II**.

Table 1. Experimental conditions, crystallographic data and details of the structure refinement for (L-ArgH$_2$)(BF$_4$)$_2$ (**I**) and (L-ArgH$_2$)(ClO$_4$)$_2$ (**II**).

Crystal	(**I**)	(**II**)
Empirical Formula	$C_6H_{16}N_4O_2^{2+}\cdot 2(BF_4^-)$	$C_6H_{16}N_4O_2^{2+}\cdot 2(ClO_4^-)$
Formula mass	349.85	375.13
Crystal system	Triclinic	Triclinic
Space group	$P1$	$P1$
a (Å)	5.5855(10)	5.60990(10)
b (Å)	6.1498(11)	6.34960(10)
c (Å)	10.234(2)	10.2927(2)
α (°)	94.574(3)	94.5820(10)
β (°)	93.618(3)	93.9040(10)
γ (°)	92.217(3)	92.0710(10)
V (Å^3)	349.37(11)	364.294(11)
Z	1	1
$\rho_{calc.}$(g cm^{-3})	1.663	1.710
2θ range, deg.	4.00 – 61.79	4.00 – 62.00
μ (mm^{-1})	0.185	0.505
F(000)	178	194
Crystal sizes, mm	0.32 x 0.26 x 0.18	0.28 x 0.26 x 0.26
Independent reflections / R_{int}	4202 / R_{int} =0.0304	4610 / R_{int} =0.0146
reflections with $I>2\sigma(I)$	3845	4600
Number of refined parameters	199	237
Completeness to theta θ, %	99.0%	100%
GOF (F^2)	1.043	1.059

reflections with $I>2\sigma(I)$	3845	4600
Flack parameter	-0.1(3)	0.051(6)
$R_1(F)$ $(I>2\sigma(I))^a$	0.0431	0.0169
$wR_2(F^2)$ (all data)^b	0.1190	0.0487
$\Delta\rho_{fin}$ (max/min) [e Å^{-3}]	0.371/-0.261	0.249/-0.245

^{a} $R_1 = \sum|F_o - |F_c||/\sum(F_o)$; ^{b} $wR_2 = (\sum[w(F_o^2 - F_c^2)^2]/\sum[w(F_o^2)^2]^{½}$

3. Results and discussion

*3.1 Crystal and molecular structures of (L-ArgH$_2$)(BF$_4$)$_2$ (**I**) and (L-ArgH$_2$)(ClO$_4$)$_2$ (**II**)*

The unit cells of both crystals contain one doubly charged *L*-ArgH$_2$ cation and two respective BF$_4^-$ or ClO$_4^-$ anions (Fig. 2). The *L*-ArgH$_2$ cation contains protonated amino and guanidyl groups and neutral carboxyl group, while in singly charged *L*-ArgH cation the carboxyl group is deprotonated and exists in form of negatively charged carboxylate group.

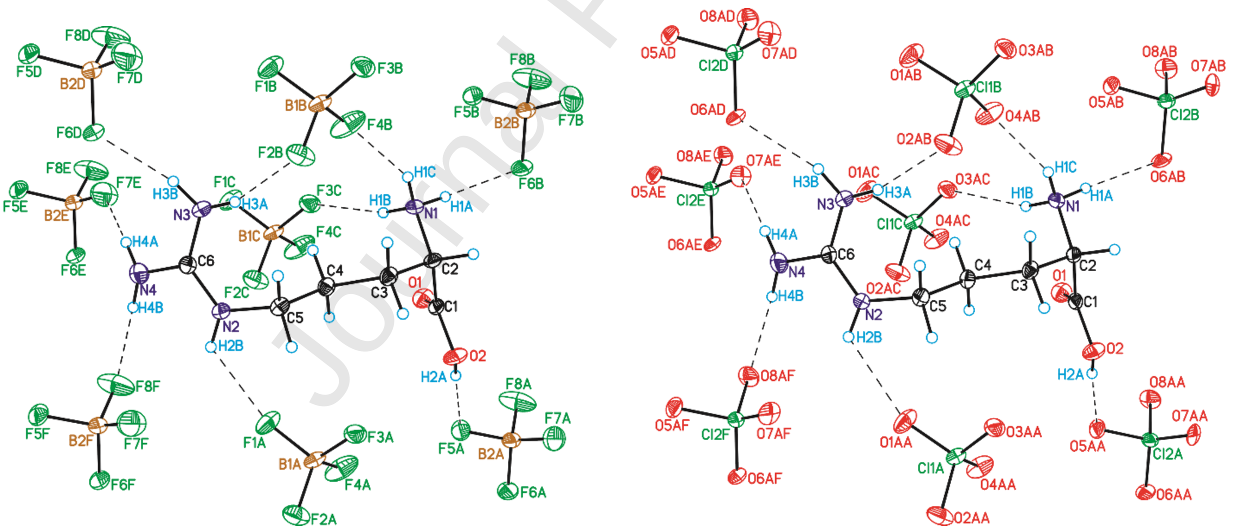

Fig. 2. General view of salts (*L*-ArgH$_2$)(BF$_4$)$_2$ (left) and (*L*-ArgH$_2$)(ClO$_4$)$_2$ (right) showing atomic numbering and H-bonding pattern. Parameters of H-bonds are provided in Tables 2 and 3. For the disordered ClO$_4$ anions, minor part is omitted for clarity. Thermal ellipsoids are drawn at 50% probability level.

Table 2. Hydrogen bond parameters (in Å and °) for (*L*-ArgH$_2$)(BF$_4$)$_2$ (**I**).

D-H···A	D-H	H···A	D···A	DHA
O2-H2A···F5A ^{i}	0.85	1.85	2.676(3)	165
N1-H1A···F6B ^{ii}	0.90	2.03	2.902(3)	163
N1-H1B···F3C ^{iii}	0.90	1.94	2.809(3)	161
N1-H1C···F4B ^{ii}	0.90	1.96	2.762(3)	147
N2-H2B···F1A ^{i}	0.90	2.32	2.983(3)	131
N3-H3A···F2B ^{ii}	0.90	2.06	2.920(3)	161
N3-H3A···F6D ^{iv}	0.90	2.07	2.932(3)	160
N4-H4A···F7E ^{v}	0.90	2.15	3.002(3)	157
N4-H4B···F8F ^{vi}	0.90	2.03	2.922(3)	173

Symmetry code: (i) x+1, y, z; (ii) x, y-1, z; (iii) x+1, y-1, z; (iv) x, y-1, z+1; (v) x+1, y-1, z+1; (vi) x+1, y, z+1.

Table 3. Hydrogen bond parameters (in Å and °) for (*L*-ArgH$_2$)(ClO$_4$)$_2$ (**II**).

D-H···A	D-H	H···A	D···A	DHA
O2-H2A···O5AA ^{i}	0.85	1.89	2.7322(13)	169
N1-H1A···O6AB ^{ii}	0.90	2.09	2.97(2)	167
N1-H1A···O6'B ^{ii}	0.90	2.09	2.944(14)	159
N1-H1B···O3AC ^{iii}	0.90	2.04	2.8729(14)	153
N1-H1C···O4AB ^{ii}	0.90	1.98	2.785(13)	147
N1-H1C···O4'B ^{ii}	0.90	2.02	2.870(10)	156
N2-H2B···O1AA ^{i}	0.90	2.44	3.090(2)	129
N3-H3A···O2AB ^{ii}	0.90	2.09	2.971(2)	165
N3-H3B···O6AD ^{iv}	0.90	2.16	3.01(2)	157
N3-H3B···O6'D ^{iv}	0.90	2.11	2.93(2)	152
N4-H4A···O7AE ^{v}	0.90	2.20	3.054(10)	159
N4-H4A···O7'E ^{v}	0.90	2.26	3.100(10)	156
N4-H4B···O8AF ^{vi}	0.90	2.10	2.992(12)	171
N4-H4B···O8'F ^{vi}	0.90	2.14	3.023(9)	168

Symmetry code: (i) x+1, y, z; (ii) x, y-1, z; (iii) x+1, y-1, z; (iv) x, y-1, z+1; (v) x+1, y-1, z+1; (vi) x+1, y, z+1.

The bond lengths C1-O1(1.210(3) Å) and C1-O2(1.325(3) Å) for the (**I**) and C1-O1(1.2064(16) Å) and C1-O2(1.3211(16) Å) for the (**II**) are expected for COOH carboxyl group. Other bond lengths of *L*-ArgH$_2$ cations in both structures also have expected values (Table 1S in Supporting Info).

The values of B-F and Cl-O bond lengths in B(1)F$_4^-$, B(2)F$_4^-$ and Cl(1)O$_4^-$, Cl(2)O$_4^-$ anions can be compared with respective values in the structures of (*L*-ArgH)(BF$_4$) [7], (*L*-ArgH)(ClO$_4$) [8] as well as in mixed salts with different anions (*L*-HisH$_2$)(NO$_3$)(BF$_4$) [21], (*L*-HisH$_2$)(NO$_3$)(ClO$_4$) [21] and (*L*-ArgH$_2$)(NO$_3$)(BF$_4$) [1], (*L*-ArgH$_2$)(NO$_3$)(ClO$_4$) [22]. The mean value of B-F bond lengths in B(1)F$_4^-$, B(2)F$_4^-$ of anions in (**I**) is equal to 1.388 Å and the mean value of Cl-O bond lengths in Cl(1)O$_4^-$, Cl(2)O$_4^-$ of anions in (**II**) is equal to 1.452 Å. In the structures of (*L*-HisH$_2$)(NO$_3$)(BF$_4$) [23] and (*L*-HisH$_2$)(NO$_3$)(ClO$_4$) [22] these values are equal to 1.389 Å and 1.429 Å, respectively, and in the structures of *L*-ArgH$_2$(NO$_3$)(BF$_4$) (fluorine atoms are disordered) [1] and *L*-Arg$H_2(NO_3)(ClO_4)$ [22] are 1.310 Å and 1.416 Å, respectively. The mean values of B-F and Cl-O bonds in the structures of (*L*-ArgH)(BF_4) [7] and (*L*-ArgH)(ClO_4) [8] are 1.31Å and 1.419 Å, respectively. The ratio of the unit cell volumes of (*L*-ArgH)(ClO_4) [8] and (*L*-ArgH)(BF_4) [7] makes 1.029. This value in case of (*L*-ArgH_2)$(ClO_4)_2$ and (*L*-ArgH_2)$(BF_4)_2$ is somewhat higher (1.043) probably due to higher impact of anions. Conformation of the (*L*-ArgH_2) cation in the structures of (**I**) and (**II**) is determined by torsion angles provided in Table 4. Similar conformations and above considered other structural features allow concluding that these crystals are isostructural that is also clearly shown by superimposition of the unit cell contents of (**I**) and (**II**) (Figure 2S in Supporting Info).

Table 4. Torsion angles [°] for (*L*-ArgH_2)$(BF_4)_2$ (**I**), (*L*-ArgH_2)$(ClO_4)_2$ (**II**) and (*L*-ArgH)(BF_4) [7], (*L*-ArgH)(ClO_4) [8].

Torsion angles	(**I**)	(**II**)	(*L*-ArgH)(BF_4)	(*L*-ArgH)(ClO_4)
O2-C1-C2-N1(ψ^1)	176.7(2)	176.31(9)	170.6(9)	167.2(4)
N1-C2-C3-C4(χ^1)	60.7(3)	60.94(12)	-165.0(9)	-161.0(4)
C2-C3-C4-C5(χ^2)	177.3(2)	178.47(10)	166(1)	166.3(4)
C3-C4-C5-N2(χ^3)	175.6(2)	176.33(9)	-178.8(9)	178.3(4)
C4-C5-N2-C6(χ^4)	-77.6(3)	-78.13(14)	85(1)	81.3(6)
N4-C6-N2-C5(χ^5)	175.5(2)	177.12(11)	-179(1)	179.8(4)

For comparison torsion angles of the (*L*-ArgH) cation in the structures of (*L*-ArgH)(BF_4) [7] and (*L*-ArgH)(ClO_4) [8] also are shown in Table 4. The conformation of the (*L*-ArgH_2) cation is somewhat folded compared to the conformation of the (*L*-ArgH) cation because of differences of χ^1 (*gauche* (g^+) in (*L*-ArgH_2) and *trans* in (*L*-ArgH) cations).

Hydrogen bonding pattern of (*L*-ArgH_2)$(BF_4)_2$ and (*L*-ArgH_2)$(ClO_4)_2$ is shown in Fig. 2. (See packing diagrams in Figures 1S, 2S in Supporting Info).

It should be noted that all nine active hydrogen atoms (those bonded to the oxygen and nitrogen atoms) are involved in H-bonding in both structures. There are also nine potential proton acceptors (eight O or F atoms from anions and C=O fragment from cation). According to empirical rule [23] it should be expected that all above enumerated centers would be involved in H-bonding. However, the C=O fragment forms no hydrogen bonds including formation of well-known C-OH…O=C bonded dimers [24]. As a result, only F (or O) atoms from the BF_4 (or ClO_4) anions participate in the hydrogen bonding system. Such crystal packing leads to an important difference between (*L*-ArgH) and (*L*-ArgH_2) cations in the structures of their salts. The

(*L*-ArgH) cations interact with each other via hydrogen bonds, while (*L*-ArgH$_2$) cations usually do not interact with each other: (*L*-ArgH$_2$)(H$_2$AsO$_4$)$_2$ [4], (*L*-ArgH$_2$)(H$_2$PO$_4$)$_2$ [25], (*L*-ArgH$_2$)(NO$_3$)$_2$ [26], (*L*-ArgH$_2$)(CF$_3$COO)$_2$ [27]. Similarly, in the structures of (**I**) and (**II**) the (*L*-ArgH$_2$) cations do not interact with each other. The (*L*-ArgH$_2$) cations in the structures of (**I**) and (**II**) form hydrogen bonds with one of two anions: O2-H2A···F5 of B(2)F_4^- anion and O2-H2A···O7 of Cl(2)O_4^- anion (see Tables 2, 3). These hydrogen bonds are relatively weak. The N(1)H_3^+ group in the structure of (**I**) forms N-H···F hydrogen bonds with two B(1)F_4^- and one B(2)F_4^- nearest anions. Similar N-H···O hydrogen bonds forms the N(1)H_3^+ group in the structure of (**II**). The protonated guanidyl groups in both structures form hydrogen bonds with the nearest anions. Many of these hydrogen bonds are weak. The (*L*-ArgH$_2$) cations and BF$_4$ and ClO$_4$ anions in the structures of (**I**) and (**II**) are located translationally along "c" axis forming infinite chains. However, no direct interactions are observed inside such chains. Cations of the same and neighboring chain interact through anions and *vice versa* thereby leading to three-dimensional H-bonded structure. In addition to hydrogen bonds shown in Fig. 2 (see also Tables 2, 3) there are also short C-H···F and C-H···O contacts which can be considered as weak hydrogen bonds: C3-H3C···F4 with C3···F4(3.208(3) Å), (H3C···F4)(2.38 Å) and ∠CHF=141°, C4-H4D···F3 with C4···F3(2.243(2) Å), H4D···F3(2.39 Å) and ∠CHF=144° in the structure of (**I**) and C3-H3C···O6 with C3···O6(3.23(1) Å) , H3C···O6(2.40 Å) and ∠CHO=141°, C4-H4D···O3 with C4···O3(3.305(1) Å), H4D···O3(2.42 Å) and ∠CHO=149° in the structure of (**II**).

*3.2 Vibrational spectra of (L-ArgH$_2$)(BF$_4$)$_2$ (**I**) and (L-ArgH$_2$)(ClO$_4$)$_2$ (**II**)*

The existence of the salts (**II**) [17] was confirmed by structural analysis. However, the knowledge of the structure allows reconsidering the vibrational data in a more detail. The infrared and Raman spectra of (**I**) (Fig. 3) and (**II**) (Fig. 4) are similar. Wavenumbers of peaks and assignment of some characteristic vibrational modes of (**I**) and (**II**) are provided in Table 2S in Supporting Info. The most characteristic and important band is ν(C=O): 1740 cm^{-1} and 1744 cm^{-1} in the IR and Raman spectra of (**I**) (Fig. 3) and 1734 cm^{-1} and 1739 cm^{-1} in the spectra of (**II**) (Fig. 4). For assignment of ν(OH) one should consider formed hydrogen bonds. For hydrogen bond O-H···O with O···O distance 2.7321 Å in the structure of (**II**) one may expect ν(OH) around 3250 cm^{-1} based on correlation between ν(OH) and R(O···O) distance [28]. The relatively broad bands in this region (at 3255 cm^{-1} in the IR spectrum of (**I**) and at 3224 cm^{-1} in the IR spectrum of (**II**)) we assign to ν(OH). The narrow absorption peaks at higher wavenumbers (at 3479, 3392, 3313 cm^{-1} and respective Raman-lines) in in the spectra of (**I**) and narrow absorption peaks at 3454, 3410, 3374, 3302 cm^{-1} and respective Raman-lines in in the spectra of (**II**) we assign to ν(NH) of NH and NH_2 groups forming relatively weak hydrogen bonds. The absorption band with peaks at 1216 and 1203 cm^{-1} we assign to stretching vibration of C-OH bond and in-plane deformation vibration of the C-O-H group. Regular tetrahedral BF_4^- and ClO_4^- anions are characterized by two stretching (symmetric and asymmetric) and two deformation (also symmetric and asymmetric) vibrations [29]. Symmetric modes (ν_s=777 cm^{-1} and δ_s=360 cm^{-1} for BF_4^- anion and ν_s=928 cm^{-1}, δ_s=459 cm^{-1} for ClO_4^- anion) are active in Raman spectrum, while asymmetric modes (ν_{as}=1070 cm^{-1} and δ_{as}=533 cm^{-1} for BF_4^- anion and ν_{as}=1119 cm^{-1} and δ_{as}=625 cm^{-1} for ClO_4^- anion) are active both in IR and Raman spectra [29]. In infrared spectra the most characteristic is the strong band caused by asymmetric stretching vibration, while in Raman spectra the most characteristic is the line caused by symmetric stretching vibration. In Fig. 3 we find the band ν_{as} at 993 cm^{-1}, which is lower than expected value and the value ν_{as}=1018 cm^{-1} of (*L*-ArgH)BF_4 [12]. In the Raman spectrum we find symmetric stretching mode of BF_4^- anion at 773 cm^{-1}, which is close to expected value and respective value 769 cm^{-1} of (*L*-ArgH)BF_4 [12]. In the infrared spectrum a band at 771 cm^{-1} is observed, which may relate to ν_s in spite that this mode is inactive in the IR spectrum for regular BF_4^- anion. The ν_{as} mode of ClO_4^- anions in the IR spectrum of (**II**) is observed as very strong band at 1044 cm^{-1}. Respective value in the spectrum of (*L*-ArgH)ClO_4 is equal to 1061 cm^{-1} [12]. The Raman-line of (**II**) caused by symmetric stretching vibration usually is very intensive. We assign the line at 943 cm^{-1} (Fig. 4) to ν_s mode because this line is absent in the Raman spectrum of (**I**) (Fig. 3). In the IR spectrum there is a peak at 928 cm^{-1}, which similarly may relate to ν_s in spite that this mode is inactive in the IR spectrum for regular ClO_4^- anion. Deformation vibrations both asymmetric and symmetric are revealed in the Raman spectrum at expected positions (629 cm^{-1} and 467 cm^{-1}). Asymmetric mode has its infrared counterpart at 626 cm^{-1}. In the Raman spectrum of (*L*-ArgH)ClO_4 the modes ν_s, δ_{as}, δ_s have 937, 629 and 461 cm^{-1} values, respectively [12]. Tentative assignment of some other peaks is shown in Table 2S.

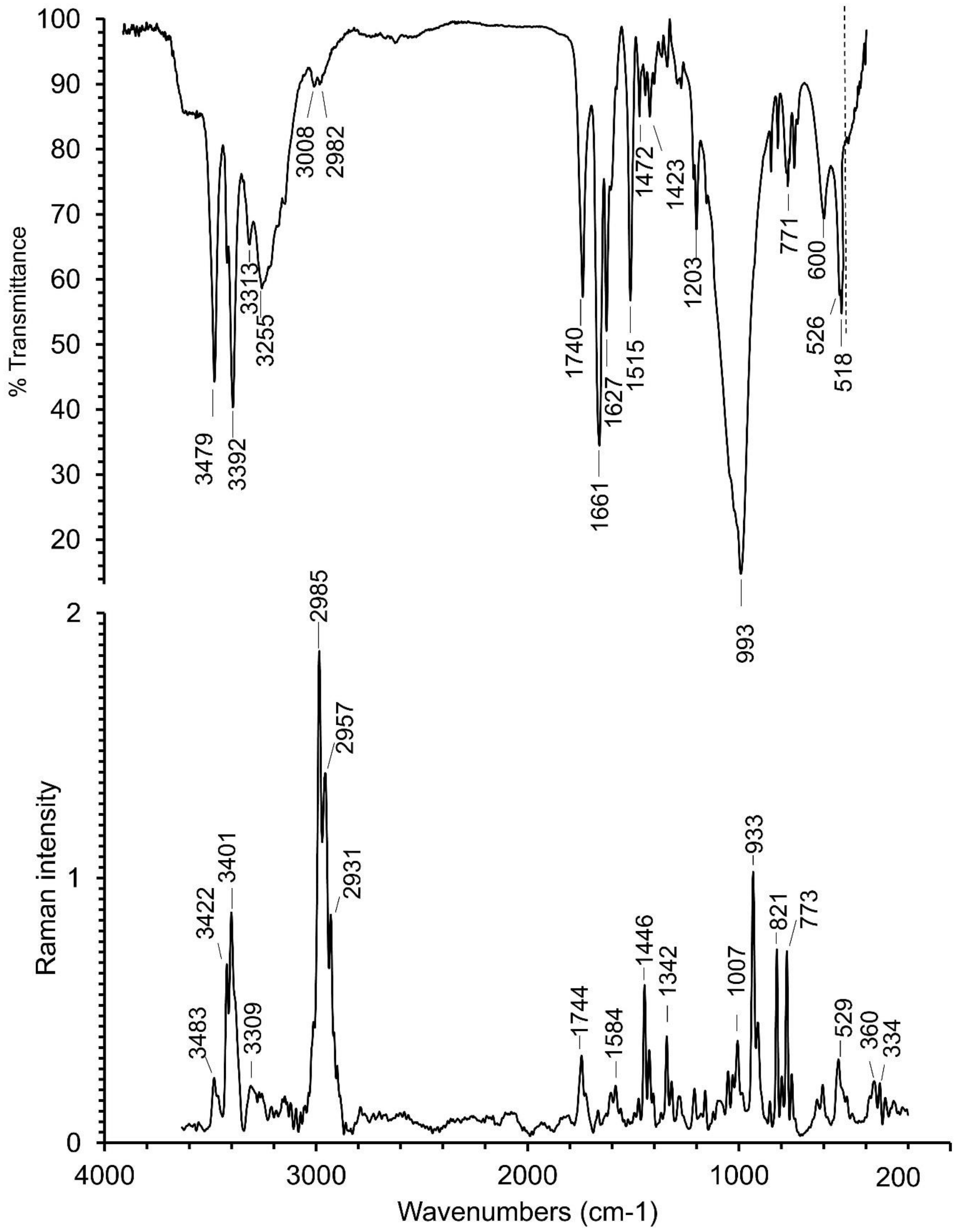

Fig. 3. Vibrational spectra of $(L\text{-ArgH}_2)(\text{BF}_4)_2$ (**I**).

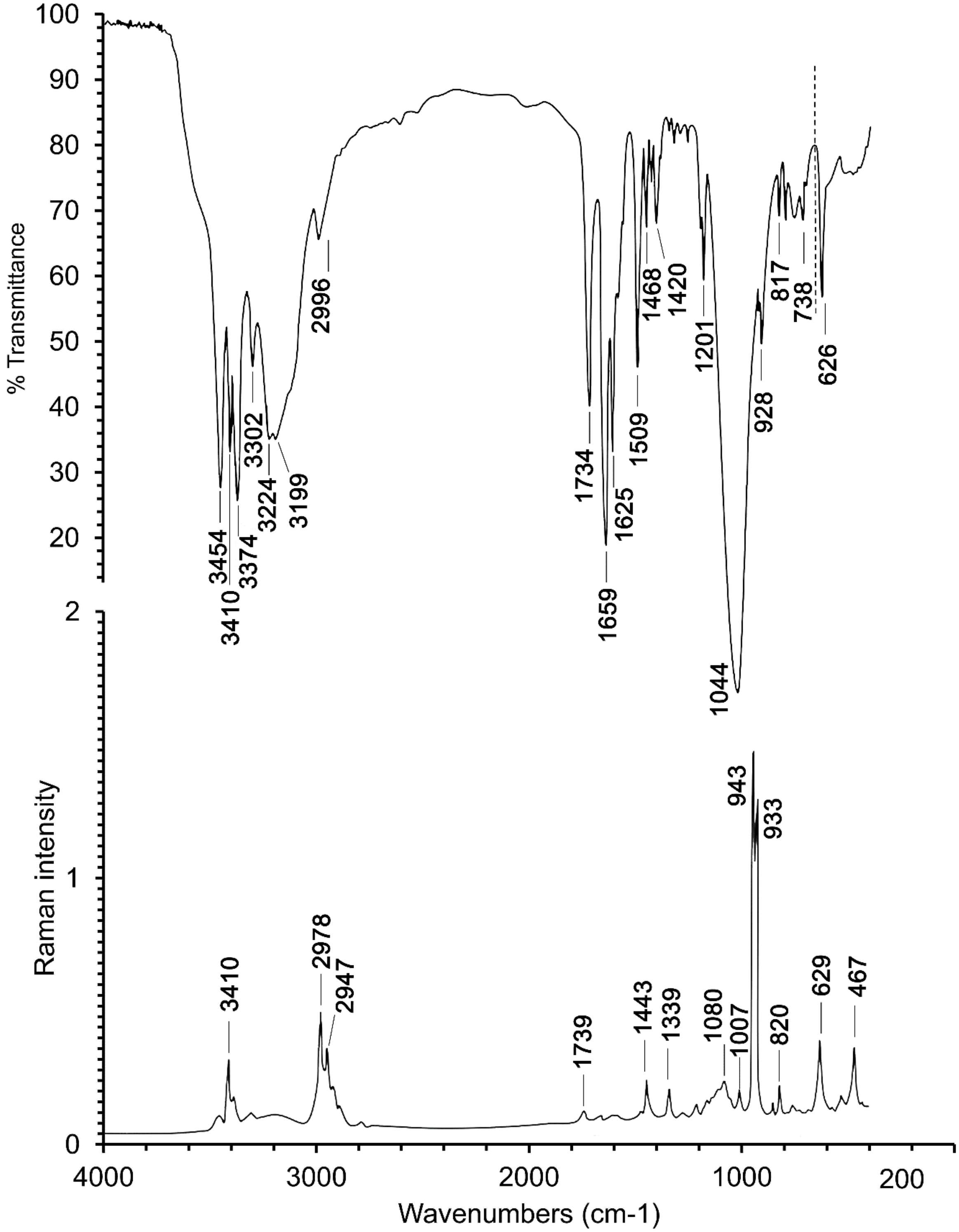

Fig. 4. Vibrational spectra of (L-ArgH_2)(ClO_4)$_2$ (**II**).

3.3 Nonlinear optical properties

Because of high hygroscopic properties of the (**I**) and (**II**) we did not investigate its nonlinear optical properties by powder method. The presence of large size crystals allowed observing second harmonic generation directly using a pulsed YAG:Nd laser. At certain orientations strong phase-matched second harmonic generation was observed.

4. Conclusions

Isostructural (*L*-ArgH$_2$)(BF$_4$)$_2$ (**I**) and (*L*-ArgH$_2$)(ClO$_4$)$_2$ (**II**) salts with doubly charged *L*-argininium(2+) cation is possible to obtain from aqueous solutions containing stoichiometric molar ratios of *L*-arginine and respective HBF$_4$ and HClO$_4$ acids in closed vessels in presence of silica gel as water vapors absorber. Structural, vibrational spectroscopic and second harmonic generation activity characterization of these crystals allowed adding the salts (**I**) and (**II**) to the existing list of salts of doubly charged *L*-argininium(2+) cation.

References

[1] M. Fleck, A.M. Petrosyan, Salts of amino acids: crystallization, structure and properties. Springer, Dordrecht, 2014, 574 p.

[2] D. Xu, M.-H. Jiang, Z.-K. Tan A new phase matchable nonlinear optic crystal – *L*-arginine phosphate monohydrate (LAP). Acta Chimica Sinica 1(1983) 230–233.

[3] S.B. Monaco, L.E. Davis, S.P. Velsko, F.T. Wang, D. Eimerl, A. Zalkin, Synthesis and characterization of chemical analogs of *L*-arginine phosphate. J. Cryst. Growth 85(1987) 252–255.

[4] A. Zalkin, D. Eimerl, S.P. Velsko, Structure of (+)-*L*-arginine diarsenate. Acta Crystallogr. C45(1989) 812–813.

[5] A.M. Petrosyan, R.P. Sukiasyan, H.A. Karapetyan, S.S. Terzyan, R.S. Feigelson, Growth and investigation of new nonlinear optical crystals of LAP family. J. Cryst. Growth 213(2000) 103–111.

[6] A.M. Petrosyan, R.S. Feigelson, E.W. Van Stryland, R.P. Sukiasyan, H.A. Karapetyan, New class of nonlinear optical crystals among arginine salts. Proc. SPIE 4751(2002) 217–222.

[7] R.-J. Wang, H.-G. Wang, J.-M. Zheng, Y.-X. Che, Crystal structure of *L*-arginine fluoroborate. Jiegou Huaxue (Chinese J. Struct. Chem.) 13(1994) 159–161.

[8] N. Srinivasan, R.K. Rajaram, Crystal structure of *L*-arginine perchlorate. Z. Kristallogr. NCS 212(1997) 311–312.

[9] C. Owens, K. Bhat, W.S. Wang, A. Tan, M.D. Aggarwal, B.G. Penn, D.O. Fraizier, Bulk growth of high quality nonlinear optical crystals of *L*-arginine tetrafluoroborate (*L*-AFB). J. Cryst. Growth 225(2001) 465–469.

[10] T. Mallik, T. Kar, Optical, thermal and structural characterization of an NLO crystal, *L*-arginine perchlorate. J. Cryst. Growth 274(2005) 251–255.

[11] A. Pricilla Jeyakumari, S. Dhanuskodi, S. Manivannan, Phase matchable semiorganic NLO material for frequency doubling: *L*-Arginine tetrafluoroborate. Spectrochim. Acta A63(2006) 91–95.

[12] A.M. Petrosyan, Vibrational spectra of *L*-arginine tetrafluoroborate and *L*-arginine perchlorate. Vib. Spectrosc. 41(2006) 97–100.

[13] S. Aruna, A. Anuradha, P.C. Thomas, M.G. Mohamed, S.A. Rajasekar, M. Vimalan, G. Mani, P. Sagayaraj, Growth, optical and thermal studies of *L*-arginine perchlorate-A promising non-linear optical single crystal. Indian J. Pure Appl. Phys. 45(2007) 524–528.

[14] S. Aruna, G. Bhagavannarayana, M. Palanisamy, P.C. Thomas, B. Varghese, P. Sagayaraj, Growth, morphological, mechanical and dielectric studies of semi organic NLO single crystal: *L*-argininium perchlorate. J. Cryst. Growth 300(2007) 403–408.

[15] D. Kalaiselvi, R.M. Kumar, R. Jayavel, Growth, optical and thermal studies of nonlinear optical *L*-arginine perchlorate single crystal. Cryst. Res. Technol. 43(2008) 645–650.

[16] D. Manimaran, C. Jesintha John, V.K. Rastogi, I. Hubert Joe, Growth and vibrational spectral investigation of nonlinear optical *L*-Argininium perchlorate-DFT study. Spectrochim. Acta A109(2013) 173–178.

[17] R.P. Sukiasyan, H.A. Karapetyan, G.G. Martirosyan, A.M. Petrosyan, *L*-arginine diperchlorate. A new salt with doubly charged cation. Proc. conf. “Laser Physics-2006”, 113–116 (2007).

[18] H.A. Petrosyan, R.A. Apreyan, A.A. Hovhannesyan, A.K. Atanesyan, A.M. Petrosyan, Nonlinear optical activity and spectroscopy of *L*-nitrohistidine monohydrate. J. Contemporary Physics (Armenian Academy of Sciences) 44(2009) 43-49.

[19] *SAINT v8.34A*. Bruker AXS Inc., Madison, Wisconsin, USA, 2013.

[20] G.M. Sheldrick, Crystal structure refinement with *SHELXL*. Acta Crystallogr. C71(2015) 3-8.

[21] A.M. Petrosyan, M. Fleck, V.V. Ghazaryan, Mixed salts of amino acids: Syntheses, crystal structure and vibrational spectra of *L*-histidinium(2+) nitrate-perchlorate and *L*-histidinium(2+) nitrate-tetrafluoroborate. Z. Kristallogr. 225(2010) 388-395.

[22] V.V. Ghazaryan, M. Fleck, A.M. Petrosyan, Mixed salts of amino acids with different anions, J. Cryst. Growth 362(2013) 182-188.

[23] (a) M.C. Etter, Encoding and decoding hydrogen-bond patterns of organic compounds. Acc. Chem. Res. 23(1990) 120-126. (b) M.C. Etter, Hydrogen bonds as design elements in organic chemistry. J. Phys. Chem. 95(1991) 4601-4610.

[24] (a) K.Yu. Suponitsky, T.V. Timofeeva, M.Yu. Antipin, Molecular and crystal design of nonlinear optical materials. Russ. Chem Rev. 75 (2006) 457-496. (b) L. Turi, J.J. Dannenberg, Molecular orbital study of crystalline acetic acid. 2. Aggregates in one, two, and three dimensions. J. Am. Chem. Soc. 116(1994) 8714-8721.

[25] S. Haussühl, H.A. Karapetyan, A.M. Petrosyan, Crystal structure and properties of *L*-arginine diphosphate. Z. Kristallogr. 218(2003) 501–506.

[26] S.S. Terzyan, H.A. Karapetyan, R.P. Sukiasyan, A.M. Petrosyan, *L*-arginine nitrates, J. Mol. Struct. 687(2004) 111–117.

[27] M.R. Silva, J.A. Paixão, A.M. Beja, *L*-Argininium bis(trifluoroacetate). Acta Crystallogr. E59(2003) 1912–1914.

[28] A. Novak, Vibrational spectroscopy of hydrogen bonded systems. In: *Infrared and Raman Spectroscopy of Biological Molecules. NATO Advanced Study Institute Series*, 43(1979) 279–303.

[29] K. Nakamoto, Infrared and Raman spectra of inorganic and coordination compounds. Part A. John Wiley and Sons Inc., 2009, 403 p.

Highlights

Crystal structure of L-argininium(2+) bis(tetrafluoroborate) has been determined

Crystal structure of L-argininium(2+) bis(perchlorate) has been determined

Infrared and Raman spectra of the obtained crystals are registered and discussed

Declaration of conflict of interest: None